4H-SiC材料中的深能级缺陷和仿真



中国科学院高能物理研究所
Institute of High Energy Physics
Chinese Academy of Sciences

2022-05-27

杨涛

4H-SiC材料中的深能级缺陷

➢ T. Kimoto等人首次在掺氮的N型4H-SiC中通过DLTS观测到$Z_{1/2}$电子缺陷。(1995)

http://aip.scitation.org/doi/10.1063/1.114800

测量材料参数表

材料	4H-SiC
生长方式	CVD
掺杂类型	N-type （氮）
掺杂浓度	3e15 - 2e16

DLTS谱

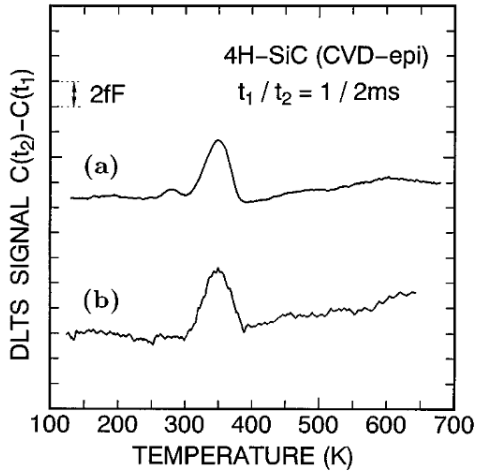


FIG. 4. DLTS spectra obtained from 4H–SiC epilayers grown on (a) (0001) Si and (b) (0001) C faces.

缺陷参数

TABLE I. Trap parameters of a deep electron trap observed in 4H–SiC epilayers by DLTS measurements.

Substrate polarity	Concentration (cm^{-3})	Activation energy (meV)	Capture cross section σ (cm^2)
Si	$3\sim5\times10^{13}$	608[a]	1×10^{-15} [a]
		665[b]	1×10^{-14} [b]
C	$1\sim8\times10^{13}$	621[a]	2×10^{-15} [a]
		679[b]	2×10^{-14} [b]

[a] $\sigma \propto T^0$
[b] $\sigma \propto T^{-2}$

$Z_{1/2}$是电子缺陷，缺陷能级Ec-0.65 eV，浓度1e13 cm^{-3}量级，俘获截面1e-14 cm^2量级

➢ C. Hemmingsson等人在2.5MeV电子辐照后的掺氮的N型4H-SiC中通过DLTS观测到电子和空穴缺陷。(1997)

http://aip.scitation.org/doi/10.1063/1.364397

测量材料参数表

材料	4H-SiC
生长方式	CVD
掺杂类型	N-type（氮）
掺杂浓度	3e14 - 1e15

DLTS谱

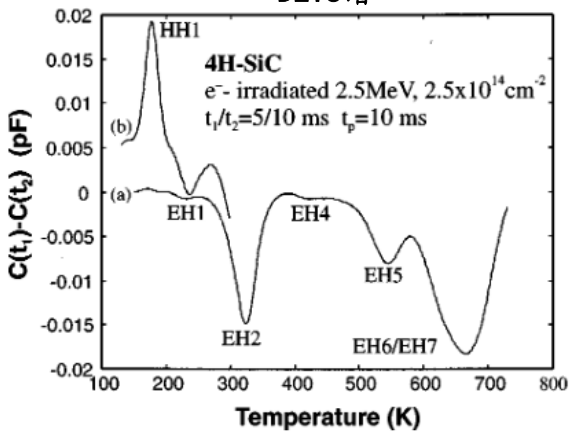


FIG. 1. DLTS spectrum observed in 4*H* SiC irradiated by 2.5 MeV electrons with a dose of 2.5×10^{14} cm^{-2} with $t_1/t_2=5/10$ ms and a pulse width of 10 ms (a) with a reverse bias of −9 V and a pulse height of 9 V and (b) with a reverse bias of −9 V and a pulse height of 12.5 V.

缺陷参数

TABLE I. The energy position E_t, trap concentration N_t, and capture cross section σ for different traps observed by DLTS in 4*H* SiC irradiated with a dose of 2.5×10^{14} cm^{-2}. σ_{inter} is estimated from the intercept of the Arrhenius plot and σ_{meas} is the measured value.

Trap level	E_t (eV)	N_t (cm^{-3})	σ_{inter} (cm^2)	σ_{meas} (cm^2)
EH1	$E_C-0.45$	2.4×10^{12}	5.0×10^{-15}	···
EH2	$E_C-0.68$	4.1×10^{13}	1.3×10^{-14}	5.0×10^{-17}
EH4	$E_C-0.72$	1.3×10^{12}	9.3×10^{-17}	···
EH5	$E_C-1.13$	1.5×10^{13}	3.5×10^{-15}	1.0×10^{-16}
EH6/EH7	$E_C-1.65$	3.9×10^{13}	2.4×10^{-13}	$>5.0\times10^{-15}$
HH1	$E_V+0.35$	1.4×10^{13}	5.4×10^{-14}	···

观测到EH2（$Z_{1/2}$）电子缺陷，缺陷能级Ec-0.68 eV，浓度4.1e13 cm^{-3},俘获截面1.3e-14 cm^2

观测到EH6/EH7 电子缺陷，缺陷能级Ec-1.65 eV，浓度3.9e13 cm^{-3},俘获截面2.4e-14 cm^2

观测到HH1 空穴缺陷，缺陷能级Ev+0.35 eV，浓度1.4e13 cm^{-3},俘获截面5.4e-14 cm^2

➢ D.Asberg等人测量低剂量(1e7-8e7 cm^{-2})B和He离子注入的N型4H-SiC外延片中的缺陷。(1999)

https://linkinghub.elsevier.com/retrieve/pii/S0921452699006018

测量材料参数表

材料	4H-SiC
生长方式	未知
掺杂类型	N-type（氮）
掺杂浓度	~1e15

DLTS谱

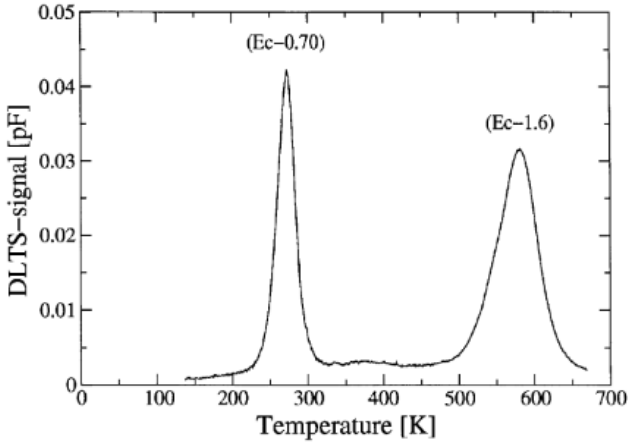


Fig. 2. DLTS temperature spectra of a sample implanted with a B dose of $3\times10^{7}\,cm^{-2}$. The measurement rate window was $\tau = 0.3125\ s^{-1}$.

DLTS随B离子注入剂量的变化

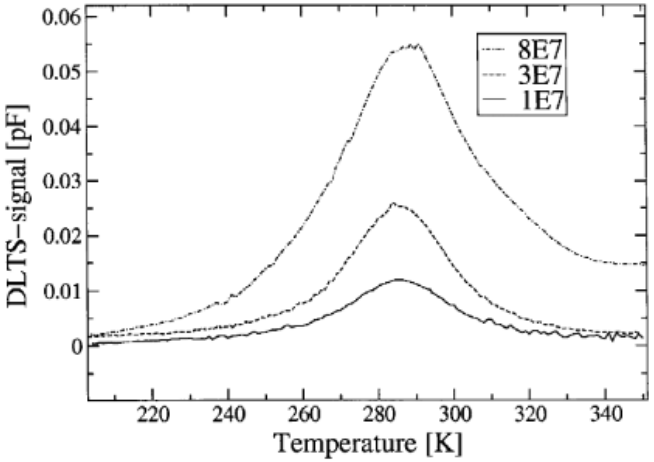


Fig. 3. DLTS temperature spectra of B implanted samples of 1×10^{7}, 3×10^{7} and $8\times10^{7}\,cm^{-2}$ (with $\tau = 1.25\ s^{-1}$).

观测到 $Z_{1/2}$ 电子缺陷，缺陷能级Ec-0.70 eV和 EH6/EH7 电子缺陷，缺陷能级 Ec-1.6 eV

观测到 $Z_{1/2}$ 电子缺陷的DLTS谱峰随B离子注入剂量的升高而升高

➢ L. Storasta等人测量(1999)研究了质子辐照后的4H-SiC中的缺陷。(2001)

http://aip.scitation.org/doi/10.1063/1.1334907

测量材料参数表

材料	4H-SiC
生长方式	CVD
掺杂类型	N-type （氮）
掺杂浓度	3.5e15-5e15

DLTS谱

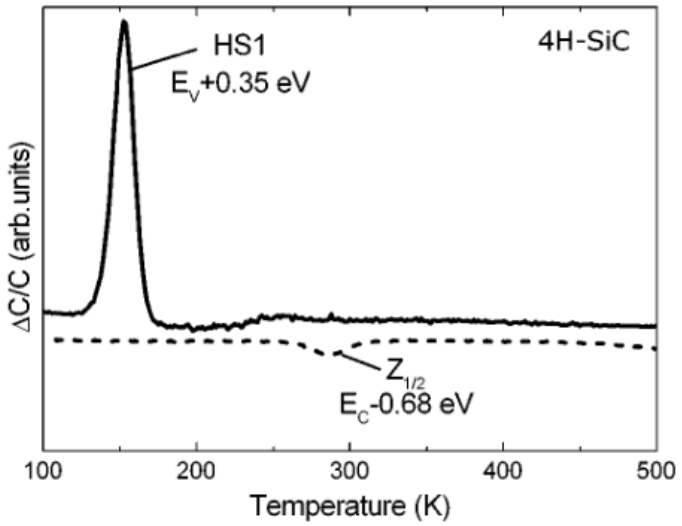


FIG. 2. DLTS and MCTS spectra for the sample irradiated with 1 $\times 10^{13}$ cm^{-2} proton dose and annealed at 1700 °C. A positive going peak reveals minority carrier (hole) trap, while a negative going peak shows the presence of majority carrier (electron) trap.

缺陷浓度随退火温度和质子辐照通量的变化

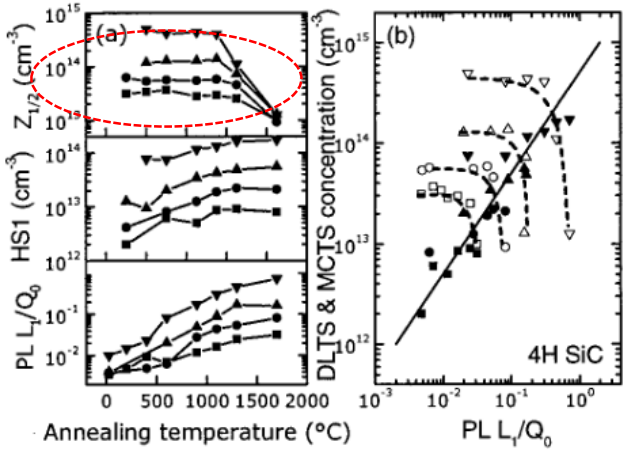


FIG. 3. (a) The annealing temperature dependence of $Z_{1/2}$, HS1, and L_1/Q_0. The proton doses used were ■ 3×10^{11}, ● 1×10^{12}, ▲ 3×10^{12}, and ▼ 1×10^{13} cm^{-2}. (b) Concentration of DLTS $Z_{1/2}$ (open symbols) and MCTS HS1 (solid symbols) against PL L_1/Q_0 ratio. The symbols used are the same as in (a) for the different proton doses. The solid and dashed lines are only guides for the eye.

观测到 $Z_{1/2}$ 电子缺陷，缺陷能级Ec-0.68 eV和 HS1空穴缺陷，缺陷能级 Ev+0.35 eV

观测到 $Z_{1/2}$ 和 HS1的缺陷浓度随质子辐照通量的增加而增加

观测到 $Z_{1/2}$ 的缺陷浓度随退火温度的升高而减小，HS1的缺陷浓度随退火温度的升高而升高

➢ J. Zhang等人研究了$Z_{1/2}$, EH6/EH7和HS1缺陷的浓度随外延生长温度的变化。(2003)

http://aip.scitation.org/doi/10.1063/1.1543240

测量材料参数表

材料	4H-SiC
生长方式	CVD
掺杂类型	N-type（氮）
掺杂浓度	3e15

DLTS谱

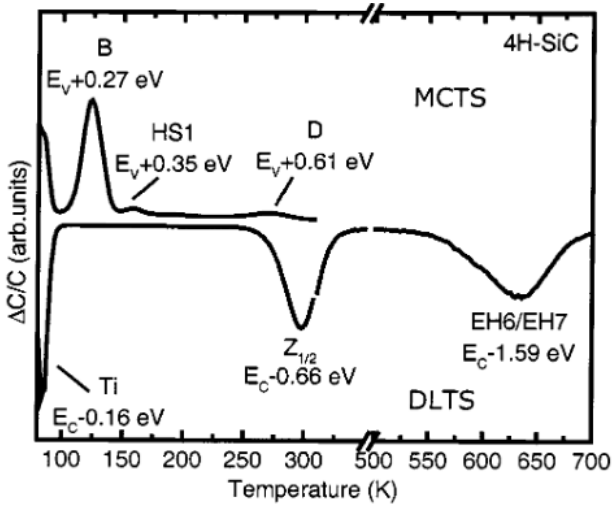


FIG. 1. DLTS and MCTS spectra recorded on a typical epilayer with a background N doping of 3×10^{15} cm^{-3}. The majority and the minority carrier traps are indicated in the DLTS and the MCTS spectra, respectively. The rate window used is 18.8 s^{-1}.

缺陷浓度随生长温度的变化

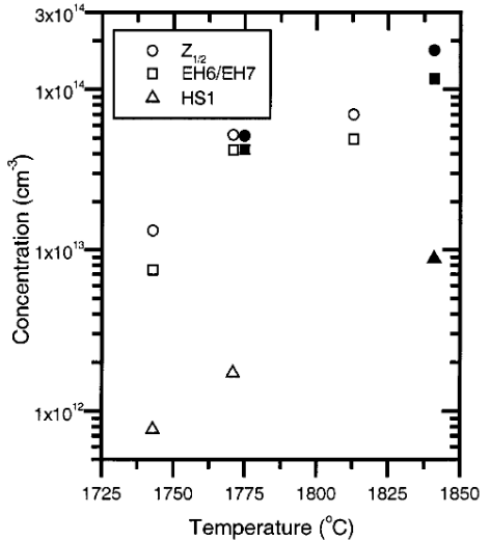


FIG. 2. Influence of the growth temperature on the concentration of the $Z_{1/2}$, EH6/7, and HS1 centers. The epilayers were grown with a C/Si ratio of 0.4. Open and filled symbols represent the chimney and inverted chimney growth conditions, respectively.

三种主要缺陷的浓度随外延生长温度的升高而增加。

J. Zhang等人总结的4H-SiC中的缺陷及其参数

TABLE I. Summary of electrical properties of the major defects observed in 4H–SiC.

Defect	Position in the band gap	Capture cross section (cm^2)
Titanium (h)	$E_C-(0.11-0.13)$ (eV)	$2\times10^{-15}-1\times10^{-14}$ (for electron)
Titanium (c)	$E_C-(0.15-0.17)$	$3\times10^{-15}-2\times10^{-14}$ (for electron)
$Z_{1/2}$	$E_C-(0.63-0.68)$	$3\times10^{-15}-2\times10^{-14}$ (for electron)
EH6/EH7	$E_C-(1.6-1.65)$	$2\times10^{-13}-9\times10^{-12}$ (for electron)
Shallow boron	$E_V+(0.23-0.28)$	$2\times10^{-14}-3\times10^{-13}$ (for hole)
HS1	$E_V+0.35$	2×10^{-14} (for hole)
D center	$E_V+(0.58-0.63)$	

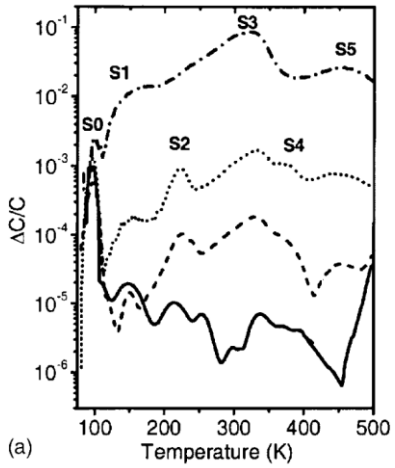
➢ Antonio Castaldini等人研究了电子和质子辐照后4H-SiC中的深能级缺陷。(2005)

http://aip.scitation.org/doi/10.1063/1.2014941

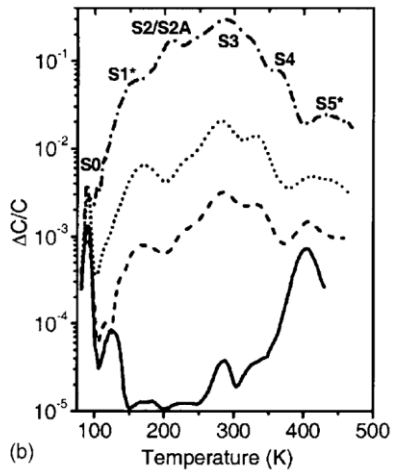
测量材料参数表

材料	4H-SiC
生长方式	CVD
掺杂类型	N-type（氮）
掺杂浓度	5e15

质子辐照前后DLTS



电子辐照前后DLTS



辐照前观测到Ti和$Z_{1/2}$缺陷，辐照后新缺陷生成，缺陷浓度与辐照通量成线性关系。

TABLE II. Enthalpy E_T, concentration N_T, apparent capture cross section σ_{inter}, and introduction rate $\eta_T = N_T/\Phi$ of the electronic levels observed in 4H–SiC irradiated with a proton fluence of 3.2×10^{13} cm^{-2}.

Trap label	E_T (eV)	N_T(cm^{-3})	σ_{inter}(cm^2)	η_T(cm^{-1})	Comparison with published data: Deep level	Comparison with published data: Attribution
S0	0.18	1.0×10^{13}	2×10^{-14}	~0	Ti,[a] P_1/P_2[b]	Ti impurity[a,c] primary defects[b]
S1	0.20	6.3×10^{13}	7×10^{-18}	3.2	…	…
S2	0.40	1.3×10^{14}	1×10^{-15}	4.1	EH1[d]	…
S3	0.72	3.5×10^{14}	2×10^{-14}	11.0	Z_1/Z_2,[a,b] EH2[d]	$N+I_C$[e]
S4	0.76	1.1×10^{14}	1×10^{-14}	3.5	EH3[d]	…
S5	1.09	7.7×10^{13}	5×10^{-13}	2.4	RD1/2,[a] EH5[d]	V_C+V_{Si}[b]

TABLE III. Enthalpy E_T, concentration N_T, apparent capture cross section σ_{inter}, and introduction rate $\eta_T = N_T/\Phi$ of the electronic levels observed in 4H–SiC irradiated with an electron fluence of 9.5×10^{14} cm^{-2}.

Trap label	E_T (eV)	N_T(cm^{-3})	σ_{inter}(cm^2)	η_T(cm^{-1})	Comparison with published data: Deep level	Comparison with published data: Attribution
S0	0.15	1.4×10^{13}	6×10^{-16}	~0	Ti,[a] P_1/P_2[b]	Ti impurity[a,c] primary defects[b]
S1*	0.23	5.5×10^{13}	9×10^{-16}	0.06	…	…
S2A	0.33	6.9×10^{14}	7×10^{-16}	0.73	…	I_C[d]
S2	0.39	4.0×10^{14}	2×10^{-15}	0.42	EH1[e]	…
S3	0.65/0.50	$4.2/5.4\times10^{14}$	$10^{-16}/10^{-14}$	0.44	Z_1/Z_2,[a,b] EH2[e]	$N+I_C$[f]
S4	0.75	2.6×10^{14}	6×10^{-15}	0.27	EH3[e]	…
S5*	0.89	4.6×10^{13}	7×10^{-15}	0.09	RD1/2,[a] EH5[e]	V_C+V_{Si}[b]

➢ P. B. Klein等人研究了$Z_{1/2}$和EH6/EH7缺陷浓度与材料厚度和少数载流子寿命的关联。(2006)

http://aip.scitation.org/doi/10.1063/1.2170144

测量材料参数表

材料	4H-SiC
生长方式	CVD
掺杂类型	N-type（氮）
掺杂浓度	~1e14

DLTS谱

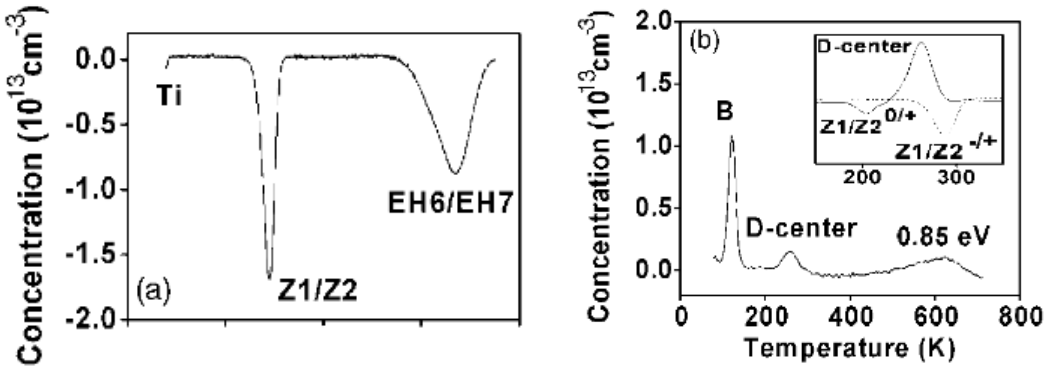
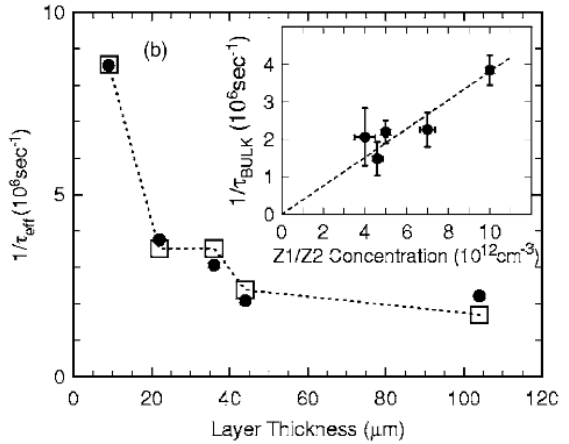


FIG. 2. Typical DLTS spectra of: (a) dominant electron traps and (b) dominant hole traps observed in n^- 4H-SiC epilayers. A Z1/Z2 (and *D*-center) spectrum measured in a *p-i-n* diode is shown in the inset.

$Z_{1/2}$缺陷浓度，少数载流子寿命和材料厚度的关系



观测到Ti，$Z_{1/2}$，EH6/EH7三种电子缺陷，B，D-center，Ev+0.85eV三种空穴缺陷

$Z_{1/2}$ 缺陷对电子和空穴都具有较大的俘获截面，主导了4H-SiC中少数载流子的寿命，其缺陷浓度与少数载流子寿命的倒数线性相关。

$$\sigma_n = 2e-14\ cm^2 \qquad \sigma_p = 3e-14\ cm^2$$

➢ P. B. Klein等人研究了热氧和退火条件对$Z_{1/2}$和EH6/EH7缺陷的影响。（2009）

https://iopscience.iop.org/article/10.1143/APEX.2.091101

测量材料参数表

材料	4H-SiC
生长方式	CVD
掺杂类型	N-type （氮）和P-type （铝）
掺杂浓度	0.9e15 - 5e15

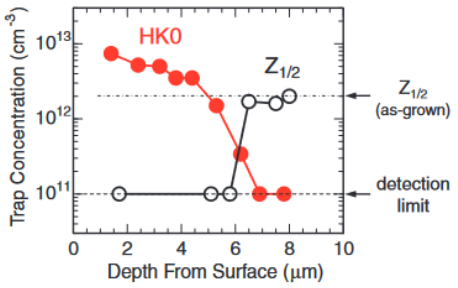


Fig. 2. Depth profiles of the concentrations of the $Z_{1/2}$ and HK0 centers in n- and p-type 4H-SiC epilayers, respectively. Both the epilayers were simultaneously oxidized at 1150 °C for 5 h.

不同热氧和退火条件下的DLTS谱

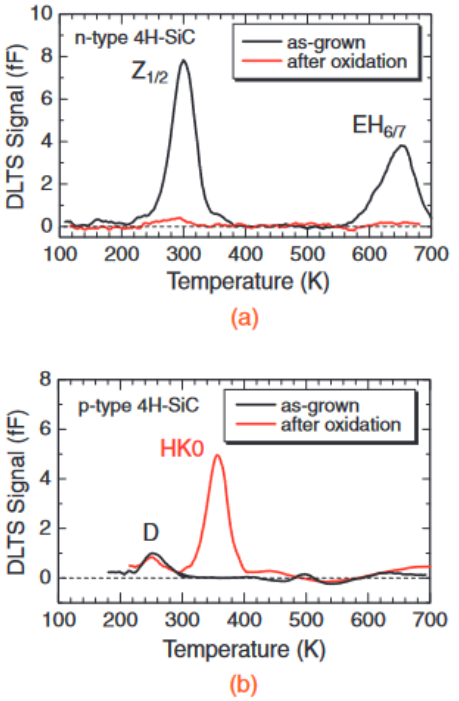


Fig. 1. DLTS spectra taken from (a) n- and (b) p-type 4H-SiC epilayers before (as-grown) and after thermal oxidation at 1150 °C for 5 h.

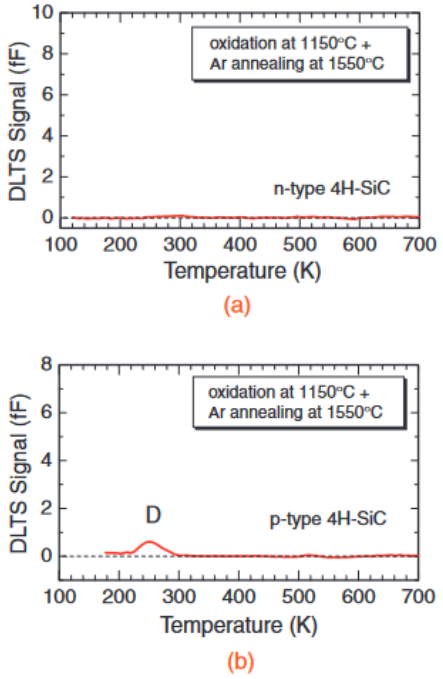


Fig. 4. DLTS spectra taken from the (a) n- and (b) p-type 4H-SiC epilayers after the two-step thermal treatment of oxidation at 1150 °C for 5 h and Ar annealing at 1550 °C for 30 min.

热氧和1550C热退火后，$Z_{1/2}$ ， EH6/EH7的缺陷浓度从1e12-1e13 cm^{-3}量级减少到了1e11 cm^{-3}以下

➢ P.B.Klein等使用TSC对比了N型掺杂和半绝缘4H-SiC中的缺陷。(2012)

10.1109/TNS.2012.2202916

测量材料参数表

材料	4H-SiC
生长方式	CVD
掺杂类型	N-type（氮）和半绝缘
掺杂浓度	3e14-8e14（N-type）

TSC谱

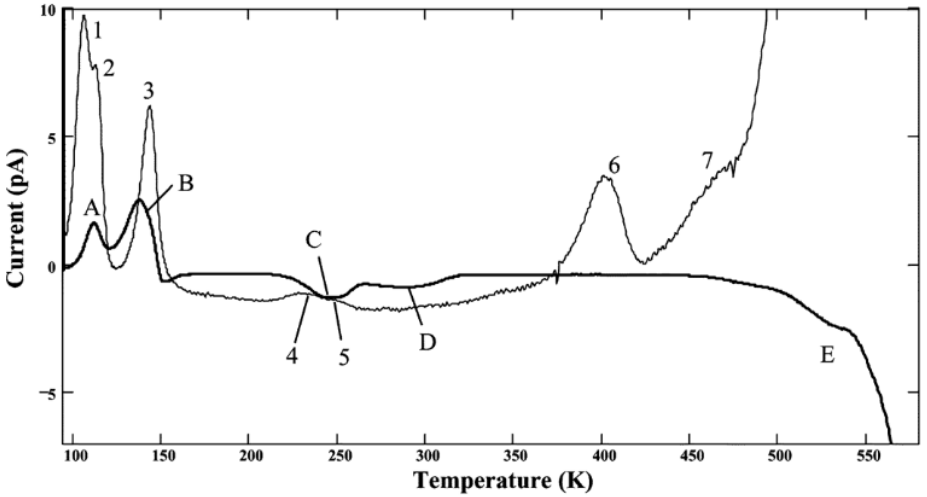


Fig. 1. TSC spectra of n-type (thin line) and SI (bold line) epitaxial layers.

缺陷参数

TABLE I
TRAP PARAMETERS DEDUCED FROM TSC MEASUREMENTS

TSC peak #	T_m @ 15 K/min (K)	Trap activation energy (eV)	Capture cross-section (cm^2)	Possible Defects or Impurities
1	106	0.22	$\sim 10^{-16}$	Al [10], [11]
2	112	0.25	$\sim 10^{-15}$	Al, B, L-center [9],[11], defect complexes
3	143	0.31	$\sim 10^{-16}$	
4	231	~0.5	-	D-center
5	250	-	-	
6	402	1.08	$\sim 4\times0^{-15}$	IL_2 [13], SI-6, SI-8 [14]]
7	~470	-	-	Unnamed [7]
A	~114	0.19	$\sim 10^{-18}$	Al, B, L-center [9], [11]
B	138-142	0.22	$\sim 10^{-19}$	
C	246-253	0.57	$\sim 2\times10^{-16}$	D-center
D	290-300	0.82-0.87	$\sim 1\times10^{-13}$	IL_1 [13], HK2 [12]
E	~525	-	-	Intrinsic defects

在两种外延片中测的缺陷既有相同也有不同

TSC的测量结果与DLTS差异较大。

have been conducted for characterization and defect correlation studies. Both epitaxial layers exhibited relatively shallow levels related to Al, B, L- and D-centers. Deep level centers in the n-type epitaxial layer peaked at ~400 K (E_a ~ 1.1 eV), and ~470 K were correlated with IL_2 defect and 1.1 eV center in high-purity bulk SI 4H-SiC. The SI epitaxial layer exhibited peak at ~290 K (E_a = 0.82–0.87 eV) that was attributed to IL_1 and HK2 centers, and at ~525 K that was related to intrinsic defects and their complexes with energy levels close to the middle of the band-gap.

➢ Krishna等研究了4H-SiC SBD探测器的性能和DLTS测量得到的缺陷。(2014)

10.1109/TNS.2014.2335736

测量样品SBD参数表

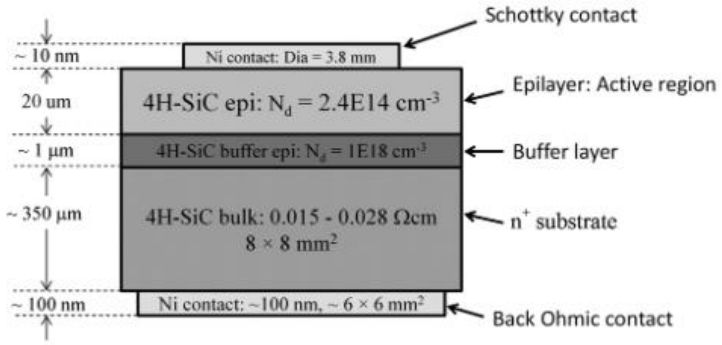


Fig. 1. n-type 4H-SiC epilayer wafer structure with Ni contacts. Figure reproduced from Ref [10].

3个样品的alpha测量能谱

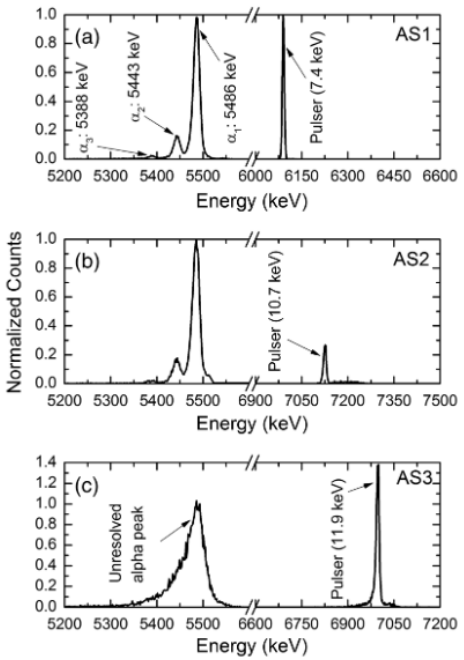


Fig. 6. Alpha pulse-height spectra obtained for detectors (a) AS1, (b) AS2, and (c) AS3 using an ^{241}Am source. The pulser spectra recorded along with has also been shown. Fig. 6(a) has been reproduced from Ref 10.

3个样品的DLTS谱

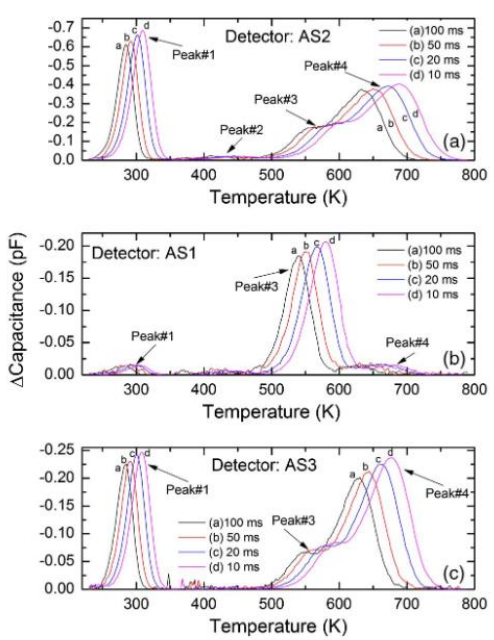


Fig. 7. DLTS scan for detectors AS2, AS1 and AS3 showing negative peaks related to electron traps present in the 4H-SiC epilayer detectors. Four correlators a, b, c and d with initial delays of 100, 50, 20, and 10 ms, respectively, were chosen to obtain different rate windows in each thermal scans ranging from 230 to 790 K.

3个样品中都观测到$Z_{1/2}$，EH6/EH7主要电子缺陷

AS3样品中的缺陷的俘获截面最大，对应器件性能最差

3个样品的测量得到的缺陷参数

Detector ID	Peak #1 Trap	$\sigma_n\times10^{-16}$ cm^2	ΔE eV	$N_t\times10^{12}$ cm^{-3}	Peak #2 Trap	$\sigma_n\times10^{-16}$ cm^2	ΔE eV	$N_t\times10^{12}$ cm^{-3}	Peak #3 Trap	$\sigma_n\times10^{-16}$ cm^2	ΔE eV	$N_t\times10^{12}$ cm^{-3}	Peak #4 Trap	$\sigma_n\times10^{-16}$ cm^2	ΔE eV	$N_t\times10^{12}$ cm^{-3}
AS1	$Z_{1/2}$	0.05	0.60	0.09	-	-	-	-	*Ci*1(?)	575	1.45	1.27	$EH_{6/7}$	68.8	1.6	0.10
AS2	$Z_{1/2}$	1.9	0.62	3.2		0.1	0.80	0.09	*Ci*1	1.7	1.31	0.93	$EH_{6/7}$	28.2	1.6	1.9
AS3	$Z_{1/2}$	28.8	0.66	1.9	-	-	-	-	*Ci*1	22.6	1.3	65	$EH_{6/7}$	158	1.6	1.8

➢ Gelczuk等研究了Al离子注入的4H-SiC SBD中DLTS测量得到的缺陷。(2014)

https://linkinghub.elsevier.com/retrieve/pii/S0038110114000239

测量材料参数表

材料	4H-SiC
生长方式	CVD
掺杂类型	N-type （氮）
掺杂浓度	1.5e16

DLTS谱

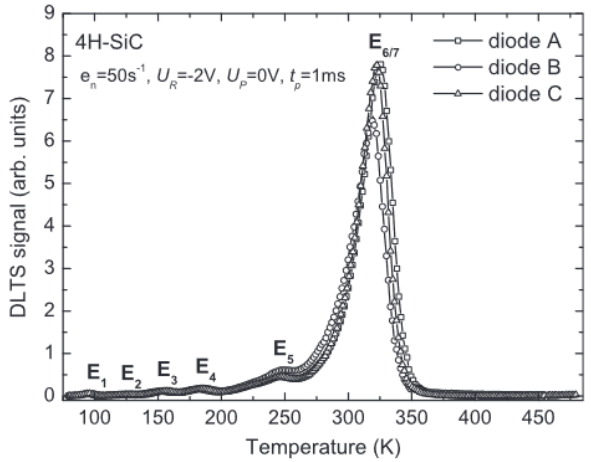


Fig. 2. DLTS spectra of 4H-SiC JBS diodes, measured with emission rate window of $e_n = 50\ s^{-1}$ and bias conditions set to: reverse voltage $U_R = -2$ V, filling pulse voltage $U_P = 0$ V and filling pulse width $t_p = 1$ ms.

Table 1
Parameters of deep electron traps revealed in 4H-SiC JBS diodes by means of DLTS measurements, i.e. activation energy ($E_a = E_C - E_T$), apparent capture cross section (σ_a), and concentration (N_T). In the last two columns, a possible attribution of traps have been made by comparing the parameters of well-known deep-level defects in 4H-SiC, as reported in the references given below.

Trap	E_a (eV)	σ_a (cm^2)	N_T (cm^{-3})	Deep level	Possible attribution
E_1	0.13	2.1×10^{-16}	8.6×10^{13}	Ti(h)[a,b]	Impurity defect
E_2	0.18	1.4×10^{-16}	5.1×10^{13}	Ti(c)[a,b], S1[c]	Impurity defect
E_3	0.23	1.6×10^{-16}	1.4×10^{14}	SE2[d]	Single plain SF
E_4	0.33	2.9×10^{-15}	1.9×10^{14}	ID_4[a], P3[a]	Intrinsic defect
E_5	0.45	1.1×10^{-15}	3.2×10^{14}	EH1[e], ID_8[a]	Intrinsic defect
$E_{6/7}$	0.68	9.7×10^{-15}	4.5×10^{15}	$Z_{1/2}$[e,f]	Intrinsic defect

样品DLTS谱中都观测5个单峰和一个双峰($Z_{1/2}$)

该样品测量得到$Z_{1/2}$ 的能级Ec-0.68eV, 缺陷浓度4.5e15 cm^{-3},俘获截面9.7e-15 cm^2

➢ Gelczuk等研究了不同氧化层覆盖的终端结器件中的缺陷。(2015)

10.1109/TNS.2015.2496902

测量样品SBD参数

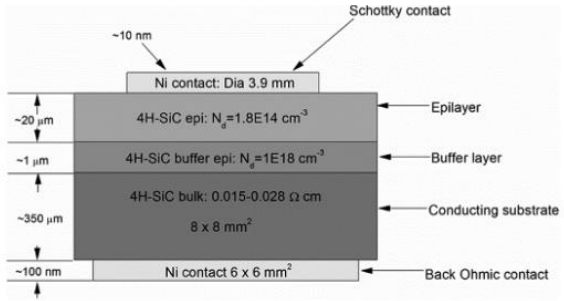


Fig. 1. Cross-sectional view of a fabricated Schottky barrier detector on 4H-SiC n-type epitaxial layer.

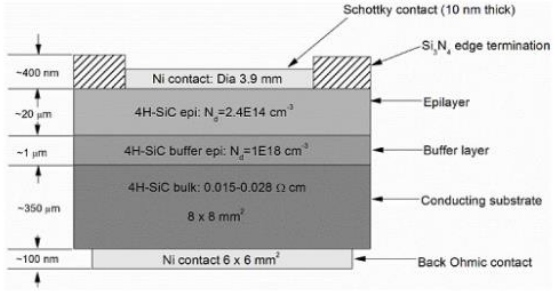


Fig. 2. Cross-sectional view of a Schottky barrier detector with edge termination. Passivating dielectric layer surrounds the Ni contact.

DLTS谱

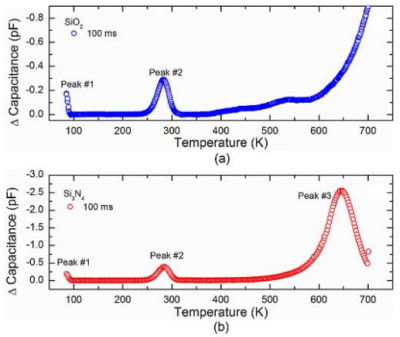


Fig. 14. DLTS scans of 2AS22 (a) and 2AS30 (b) are shown with negative peaks corresponding to electron traps in the detector up to 700 K. Only a single rate window is shown (50 ms, 20 ms, and 10 ms not shown).

TABLE II
DEFECT PARAMETERS OBTAINED FROM DLTS SCANS

Det ID	Peak #1				Peak #2				Peak #3				Peak #4			
	Trap	$\sigma_n\times$ 10^{-14} cm^2	ΔE eV	$N_t\times$ 10^{12} cm^{-3}	Trap	$\sigma_n\times$ 10^{-16} cm^2	ΔE eV	$N_t\times$ 10^{12} cm^{-3}	Trap	$\sigma_n\times$ 10^{-17} cm^2	ΔE eV	$N_t\times$ 10^{12} cm^{-3}	Trap	$\sigma_n\times$ 10^{-16} cm^2	ΔE eV	$N_t\times$ 10^{12} cm^{-3}
2AS1a	Ti(c)	7.06	0.19	2.52	$Z_{1/2}$	5.04	0.62	4.16	EH_6	552	1.40	1.04	EH_7	1.73	1.45	1.34
2AS22	Ti(c)	9.84	0.20	3.16	$Z_{1/2}$	13.8	0.64	3.56	-	-	-	-	-	-	-	-
2AS30	Ti(c)	0.47	0.22	2.14	$Z_{1/2}$	7.24	0.63	3.16	Ci1	0.58	1.25	18.3	-	-	-	-

2AS1a (without edge termination), 2AS22 (SiO2 edge termination), and 2AS30 (Si3N4 edge termination).

观测到Ti，$Z_{1/2}$ ，EH6/EH7三种电子缺陷

DLTS测量结果表明Si3N4的终端结能够有效降低$Z_{1/2}$缺陷的浓度

➢ Mohammad等研究了不同退火温度对4H-SiC SBD中缺陷浓度和俘获截面的影响。(2016)

10.1109/TNS.2016.2535212

测量样品SBD参数

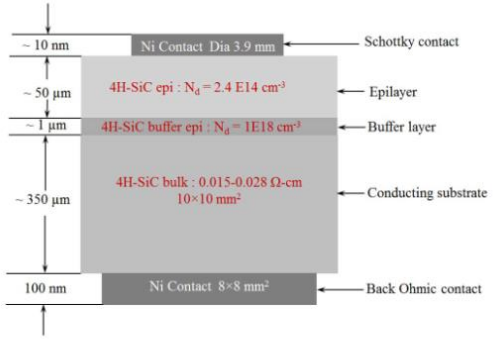


Fig. 1. Schematic diagram of the cross-sectional view of 50 μm-thick n-type 4H-SiC Schottky barrier device.

DLTS谱

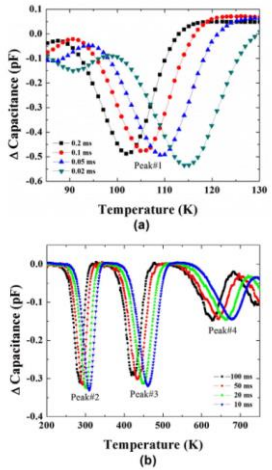


Fig. 2. DLTS spectra obtained using the 50 μm-thick n-type Ni/4H-SiC epitaxial Schottky barrier in a temperature range: (a) 85 K - 130 K with a smaller set of initial delays and (b) 200 K - 750 K with a larger set of initial delays.

测量得到的4种缺陷的俘获截面和浓度与退火温度的关系

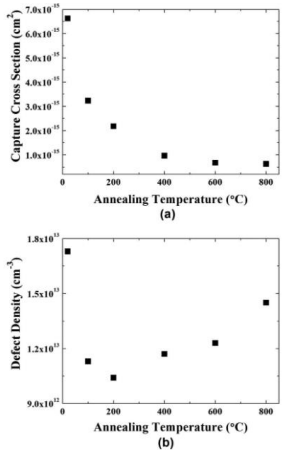


Fig. 5. Defect (E_C-0.16 eV corresponding to peak #1) parameters variation with annealing temperature: (a) capture cross-section and (b) defect density.

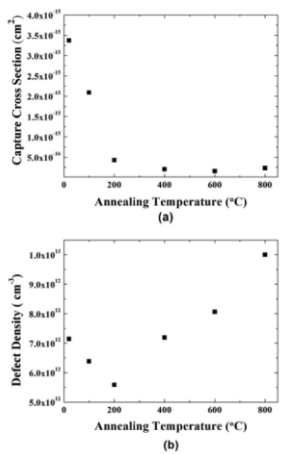


Fig. 7. Defect $Z_{1/2}$ (corresponding to peak #2, E_C-0.67 eV) parameters variation with annealing temperature: (a) capture cross-section and (b) defect density.

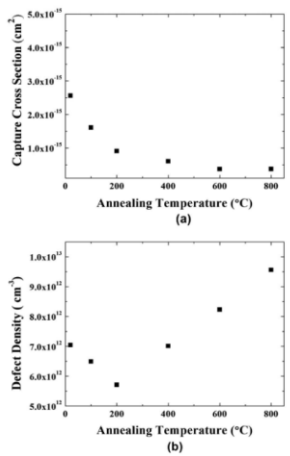


Fig. 8. Defect EH_5 (corresponding to peak #3, E_C-1.03 eV parameters variation with annealing temperature: (a) capture cross-section and (b) defect densitv.

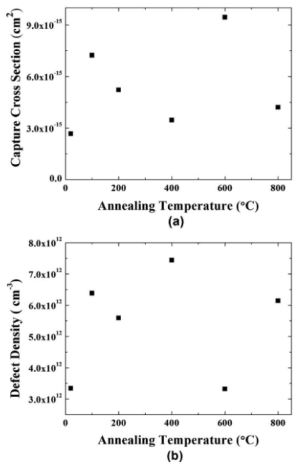


Fig. 9. Defect $EH_{6/7}$ (corresponding to peak #4, E_C-1.6 eV) parameters variation with annealing temperature: (a) capture cross-section and (b) defect density.

观测到Ti，$Z_{1/2}$ ，EH5，EH6/EH7四种电子缺陷

缺陷参数

TABLE I
DEFECT PARAMETERS OBTAINED FROM THE DLTS MEASUREMENTS

Peak #	σ cm^2	ΔE eV	N_t cm^{-3}	Possible Trap Identity
Peak 1	6.62×10^{-15}	$E_c-0.17$	1.7×10^{13}	Ti(c)[a]
Peak 2	3.37×10^{-15}	$E_c-0.67$	7.1×10^{12}	$Z_{1/2}$[b]
Peak 3	5.56×10^{-17}	$E_c-1.04$	7.1×10^{12}	EH_5[c]
Peak 4	2.66×10^{-17}	$E_c-1.60$	3.3×10^{12}	$EH_{6/7}$[d]

Ti，$Z_{1/2}$ ，EH5三种缺陷的俘获截面随退火温度的升高而降低，浓度随退火温度的变化趋势相似(先降后升)。

➢ Yawei He等研究了整片4H-SiC 外延晶圆上的$Z_{1/2}$缺陷分布。(2020)

https://linkinghub.elsevier.com/retrieve/pii/S0022024819305676

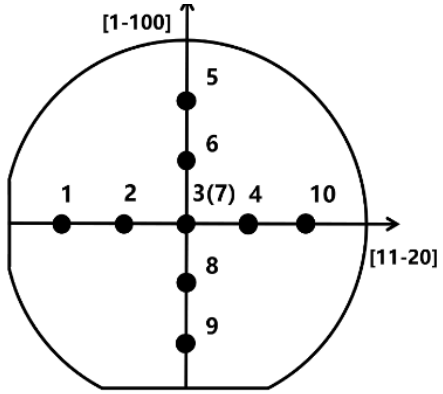


Fig. 1. The locations of nine sample points on the wafer.

测量样品SBD参数

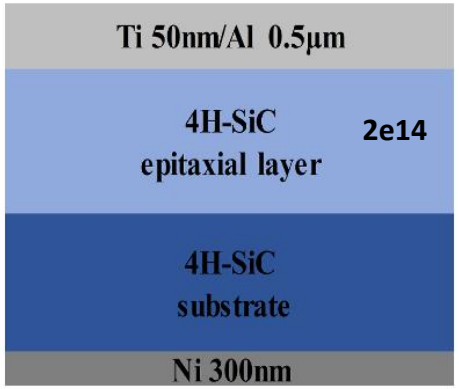


Fig. 2. Schematic diagram of Schottky structure of the samples.

DLTS谱

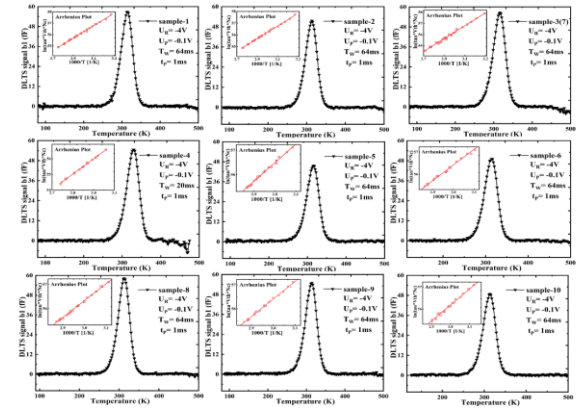
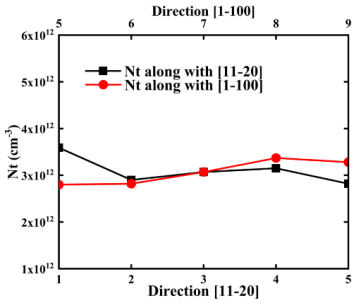


Fig. 3. DLTS signal spectrums of nine samples at the temperature range from 80 K to 500 K. Sample-1 ~ sample-10 corresponds to the nine sample points in Fig. 1. Inset: Arrhenius Plots are obtained from the fitted curves.

缺陷浓度分布



. 4. The concentrations of $Z_{1/2}$ defects distribute in the direction of [11–20] d [1–100].

掺杂浓度分布

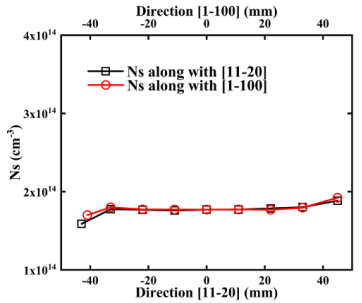


Fig. 5. The effective doping concentration of the epitaxial layer in the direction of [11–20] and [1–100].

缺陷参数

Table 1
The deep level information of nine Schottky structures.

	sample-1	sample-2	sample-3(7)	sample-4	sample-5	sample-6	sample-8	sample-9	sample-10
Energy (eV)	0.673	0.662	0.607	0.667	0.658	0.660	0.666	0.689	0.630
Sigma (cm^2)	4.60E-15	3.24E-15	4.17E-16	3.91E-15	2.27E-15	2.93E-15	4.03E-15	8.16E-15	1.29E-15
Nt (cm^{-3})	3.59E + 12	2.90E + 12	3.07E + 12	3.15E + 12	2.80E + 12	2.82E + 12	3.37E + 12	3.28E + 12	2.82E + 12

只观测到$Z_{1/2}$ 电子缺陷

$Z_{1/2}$ 缺陷在整块晶圆上浓度存在差异，但差异很小，分布均匀。

4H-SiC中实验观测到，辐照前后都存在的深能级缺陷：

名称	电极性	能级	俘获截面 [cm^2]	原生缺陷浓度[cm^{-3}]
Ti	Acceptor	(Ec-0.12 eV) ~ (Ec-0.22 eV)	(1e-14 ~1e-13) for electron	1e12 ~ 1e13
$Z_{1/2}$	Acceptor	(Ec-0.62 eV) ~ (Ec-0.68 eV) (Ec-0.67eV)	(1e-15 ~1e-13) for electron $\sigma_n = 2e-14 \quad \sigma_p = 3e-14$	1e12 ~ 1e15
$EH_{6/7}$	Acceptor	(Ec-1.25 eV) ~ (Ec-1.73 eV)	(1e-17 ~1e-15) for electron	1e12 ~ 1e13
HS1(HH1)	Donor	(Ev+0.35 eV)	(1e-14 ~1e-13) for hole	1e12 ~ 1e14
D-center	Donor	(Ev+0.58 eV) ~(Ev+0.63 eV)	-	-

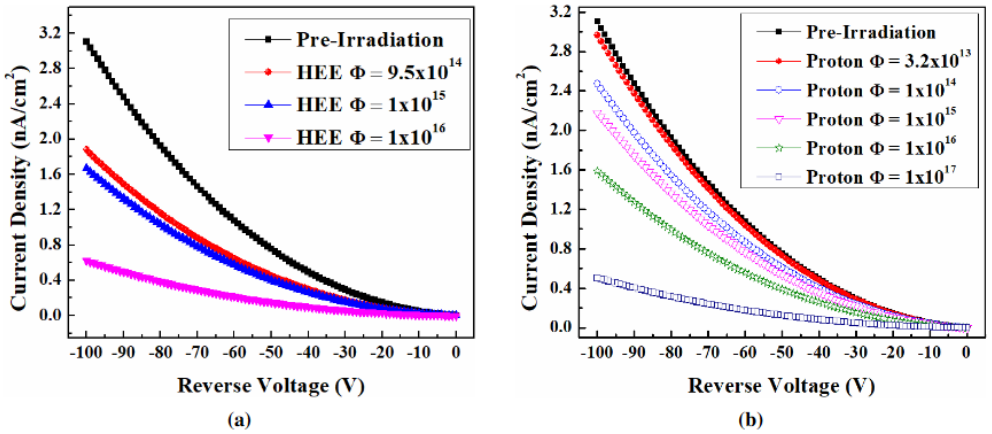
4H-SiC的深能级缺陷仿真

Silvaco TCAD 缺陷仿真

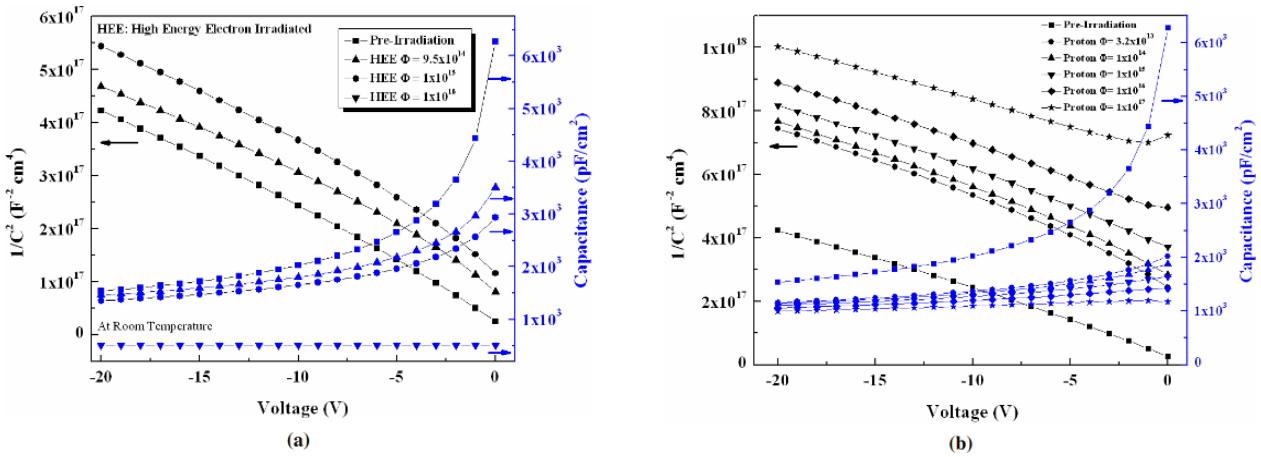
➢ S. Tripathi等仿真了4H-SiC SBD在电子和质子辐照前后电流和电容的变化

https://iopscience.iop.org/article/10.1088/1748-0221/14/02/P02002 *该仿真中使用的缺陷参数见p8

漏电流在辐照前后的仿真



电容在辐照前后的仿真



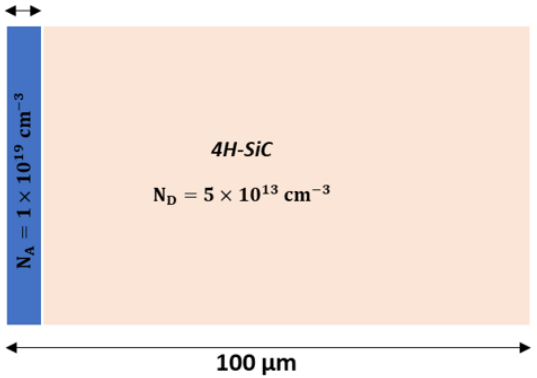
- 漏电流随辐照通量的增加(缺陷浓度增加)而减小 -> 电阻增大
- 电容仿真表明类受主缺陷的引入补偿了施主 -> 施主移除

Sentaurus TCAD 缺陷仿真

Sentaurus TCAD 缺陷仿真：

- 仿真目的：研究现有可测量到的缺陷在数值仿真中对SiC器件电流和电容的影响。寻找**辐照前**对PIN器件反向漏电流提升最大的缺陷。

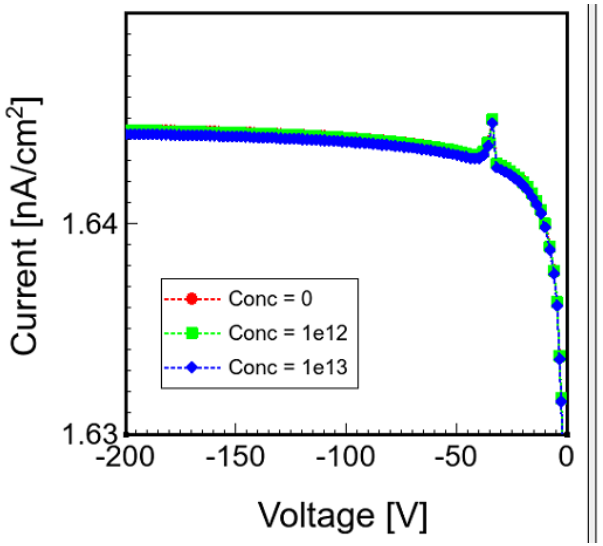
- 器件结构采用100um 4H-SiC PIN,缺陷均匀分布在4H-SiC材料中，对单个缺陷的效果逐一仿真电流电压和电容电压曲线，缺陷截面和浓度参考文献中的测量值。



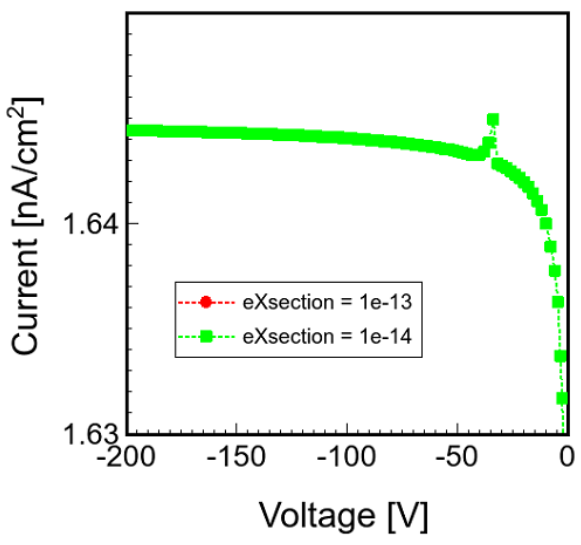
Ti缺陷对漏电流和电容的影响

名称	电极性	能级	俘获截面 [cm^2]	原生缺陷浓度[cm^{-3}]
Ti	Acceptor	(Ec-0.12 eV) ~ (Ec-0.22 eV)	(1e-14 ~1e-13) for electron	1e12 ~ 1e13

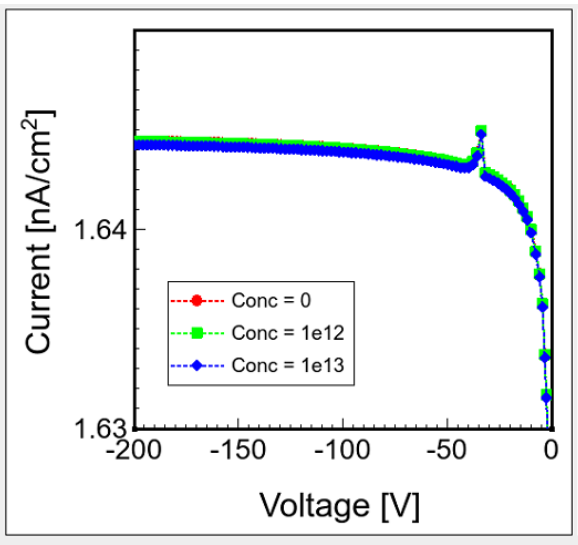
缺陷浓度对电流的影响



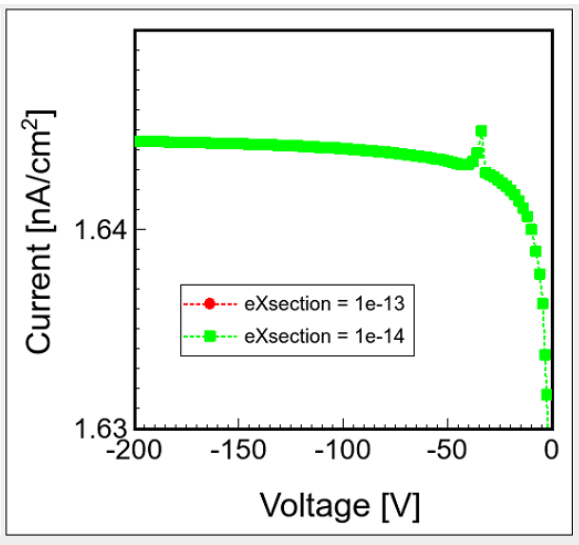
俘获截面对电流的影响



缺陷浓度对电容的影响



俘获截面对电容的影响

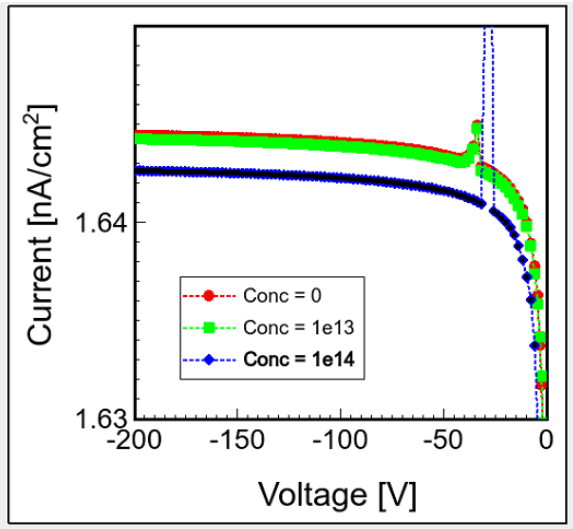


Ti作为浅受主缺陷，对施主的补偿作用微弱，对电流和电容的影响无影响。

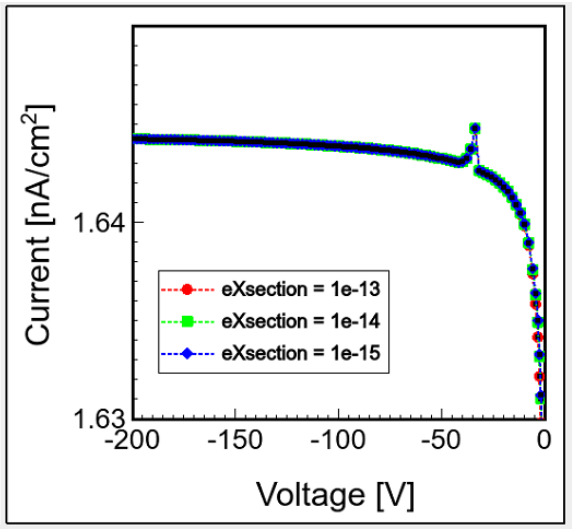
$Z_{1/2}$缺陷对漏电流和电容的影响

名称	电极性	能级	俘获截面 [cm^2]	原生缺陷浓度[cm^{-3}]
$Z_{1/2}$	Acceptor	(Ec-0.62 eV) ~ (Ec-0.68 eV) (Ec-0.67eV)	(1e-15 ~1e-13) for electron $\sigma_n = 2e-14 \quad \sigma_p = 3e-14$	1e12 ~ 1e15

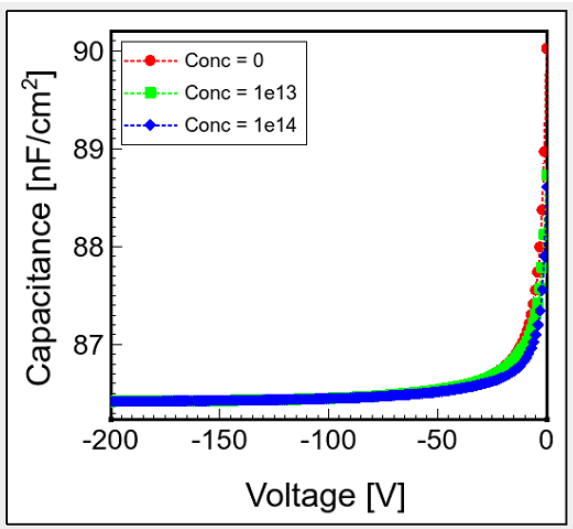
缺陷浓度对电流的影响



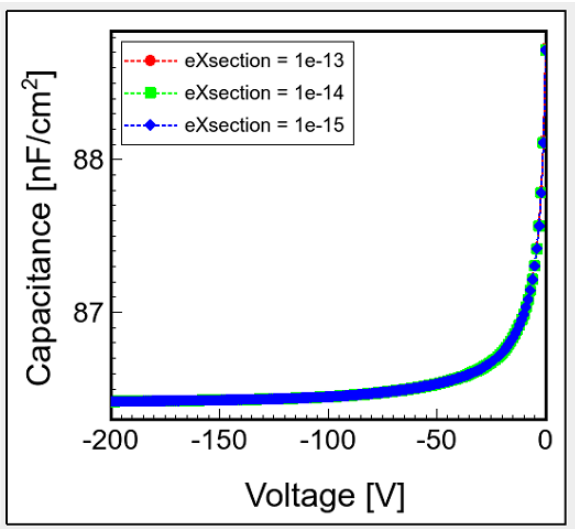
俘获截面对电流的影响



缺陷浓度对电容的影响



俘获截面对电容的影响

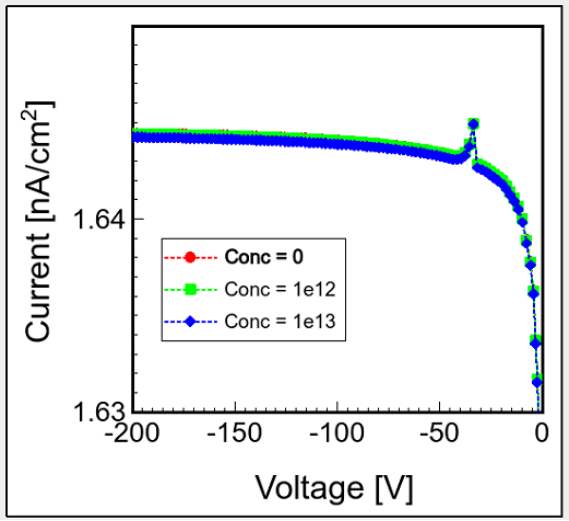


相比于Ti，$Z_{1/2}$能级更深，作为浅受主缺陷，对施主的补偿作用明显。在N型SiC中对电阻的影响主导了反向漏电流的减小。

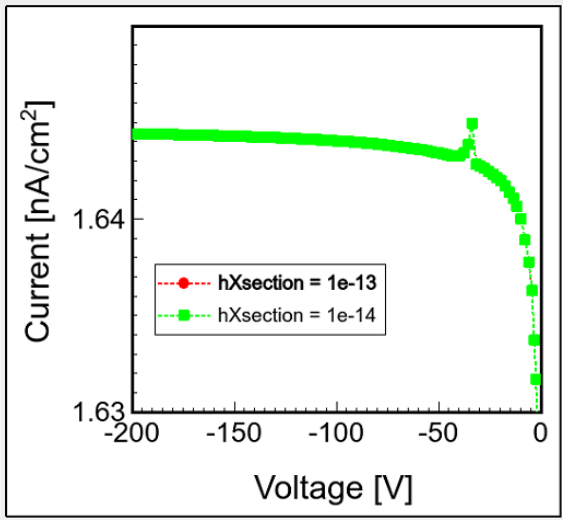
➢ HS1缺陷对漏电流和电容的影响

名称	电极性	能级	俘获截面 [cm^2]	原生缺陷浓度[cm^{-3}]
HS1(HH1)	Donor	(Ev+0.35 eV)	(1e-14 ~1e-13) for hole	1e12 ~ 1e14

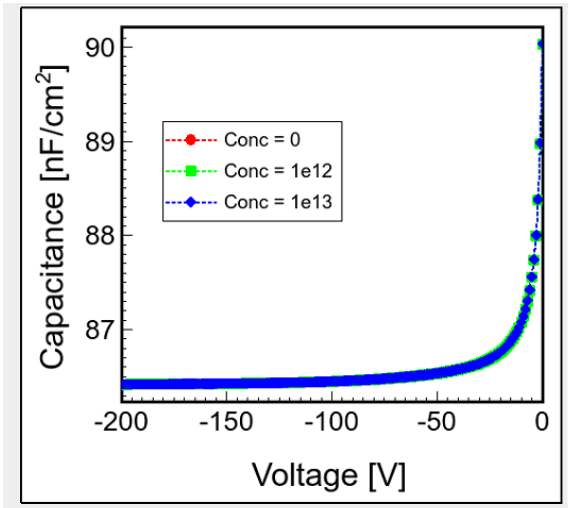
缺陷浓度对电流的影响



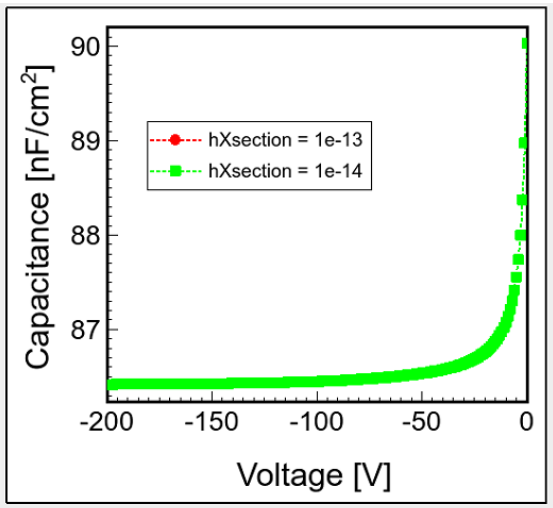
俘获截面对电流的影响



缺陷浓度对电容的影响



俘获截面对电容的影响



HS1作为浅施主缺陷，在N型SiC中对电阻有微弱的影响。对电容和漏电流的影响很小。

Sentaurus TCAD 仿真总结：

- 在TCAD数值仿真中，DLTS观测到的Ti和Z1/2电子缺陷对电流和电容的影响由类受主缺陷补偿机制主导。缺陷的增加，漏电流减小。

- 在TCAD数值仿真中，DLTS观测到的HS1空穴缺陷对电流和电容的影响很小。

- 浅能级缺陷对电容和电流的影响微弱，需要研究更深能级EH6/7等缺陷的影响。（缺陷参数的确定和计算的收敛性问题）

